

# Significance of blade element theory in performance prediction of marine propellers

Ernesto Benini \*

*Department of Mechanical Engineering, University of Padova, Via Venezia, 1, 35131 Padova, Italy*

Received 8 July 2003; received in revised form 12 November 2003; accepted 3 December 2003

---

## Abstract

This paper illustrates the implementation of a combined momentum-blade element theory for light and moderately loaded marine propellers and highlights its relevance, when compared to other more complex procedures, for their design and analysis. For this purpose, the results obtained using the theoretical model are first validated against experimental data concerning four Wageningen B-series propellers, and then these results are compared to those found using a fully three-dimensional Navier–Stokes calculation. The reasons of the differences in the results are analyzed and discussed using theoretical arguments.

© 2004 Elsevier Ltd. All rights reserved.

*Keywords:* Blade element theory; Propellers; Navier–Stokes equations

---

## 1. Introduction

Propeller theories have considerably improved during the past decades and today several methods are available for propeller design and analysis based on different levels of sophistication. At the top of this hierarchy we probably find the three-dimensional viscous flow models, where the three-dimensional incompressible Reynolds-averaged Navier–Stokes (RANS) equations are implemented and solved iteratively. Following are the lifting surface methods, the most advanced of which incorporate RANS equations to account for the viscous effects near the blade walls (Black, 1997). While the use of lifting surface methods is a well-renewed technique being in use since a long time, examples of application of the RANS equations are found only in the most recent scientific literature, see for instance the works of

---

\* Tel.: +39-049-8276799; fax: +39-049-8276785.

E-mail address: [ernesto.benini@unipd.it](mailto:ernesto.benini@unipd.it) (E. Benini).

### Nomenclature

$a$	axial induction factor
$a'$	tangential induction factor
$B$	number of blades
$c$	chord (m)
$C_D$	drag coefficient
$C_L$	lift coefficient
$C_p$	pressure coefficient = $(p - p_0)/(0.5\rho W^2)$
$D$	drag (N)
$D$	propeller diameter (m)
$J$	advance coefficient = $V_A/(nD)$
$K, K_\epsilon, K_\beta$	Goldstein–Tachmindji correction factors
$K_Q$	torque coefficients
$K_T$	thrust coefficient
$L$	lift (N)
$n$	rotational velocity (rps)
$P$	pitch (m)
$p$	pressure (Pa)
$p_0$	pressure of undisturbed flow (Pa)
$Q$	torque (Nm)
$r$	local radius (m)
$R$	propeller radius (m)
$r_{\text{boss}}$	propeller boss radius (m)
$T$	thrust (N)
$V_A$	speed of advance (m/s)
$V_r$	radial component of flow velocity (m/s)
$W$	relative velocity (m/s)

### Greek symbols

$\alpha$	incidence angle (deg)
$\beta_i, \beta, \beta_\epsilon$	angle of relative velocity at domain inlet, at propeller and at domain outlet (deg)
$\phi$	stagger angle (deg)
$\eta$	propeller open-water efficiency
$\rho$	density (kg/m <sup>3</sup> )
$\Omega$	rotational velocity (s <sup>-1</sup> )

Hsiao and Pauley (1998), Martinez-Calle et al. (2002), Feng et al. (1998) and Chen and Stern (1999). Using methods of this type good agreement with experimental results for blade pressure distribution and open-water characteristics has been achieved. However, such methods are difficult to be implemented and require so much computational resources that are not as easily applied to the iterative

geometry manipulation, which characterizes the design process. A much simpler approach, based on variants of the so-called “modified blade element theory” (MBET), is inherently two-dimensional and collocates close to the bottom of the above hierarchy, especially as far as complexity and computational effort are concerned. Thus, it is considered to be an effective tool during the design process even though it is based on simplifying hypothesis.

The MBET theory is based on the assumption that each streamtube passing through the screw disc can be analyzed independently from the rest of the flow. Therefore, the variations in the fluid dynamic quantities occur in the meridional plane along the axial and radial directions from strip to strip, without taking expressly into account the radial equilibrium among the strips. Such hypothesis is realistic when the circulation distribution over the blade is relatively uniform, i.e. in absence of control surfaces that represent radial discontinuities in the blade loading. In these circumstances, the largest part of the shed vorticity produced by the blades is confined at the hub and, above all, at the tip. The second hypothesis of the strip theory is that the radial components of the flow velocity are negligible everywhere within the fluid volume, i.e. the flow is supposed to be two-dimensional. Consequently, the results of two-dimensional cascade tests, obtained both experimentally and numerically, can be used to predict the hydrodynamic forces exerted by the fluid on each blade element. Also, when the screw blades have a non-zero rake angle (i.e. the screw blades are not perpendicular to the axis of rotation), the velocity component along the radius is neglected. Furthermore, the theory does not include secondary effects such as three-dimensional flow velocities induced on the propeller by the shed tip vortex or radial components of flow induced by angular acceleration due to the rotation of the propeller. In comparison with real propeller results, this theory is known to over-predict thrust and under-predict torque with a resulting increase in theoretical efficiency of 5–10%. For this reason, a tip-loss correction model is often included that is able to improve performance prediction. Moreover, the MBET leads to incorrect results for extreme conditions when the flow on the blade becomes massively stalled. In spite of these limitations, the MBET theory has been found very useful for comparative studies such as optimizing blade pitch setting for a given cruise speed or in determining the optimum blade solidity for a propeller. Given the above limitations, it is still the best tool available to get good first order predictions of thrust, torque and efficiency for propellers under a large range of operating conditions.

In this paper, a particular implementation of the blade element theory for marine propellers is proposed. The particularity relies on the fact that the properties of each blade profile are calculated numerically within the solution procedure, using a panel/integral boundary layer method (IBLM), and are not postulated a priori as done in traditional approaches. In this way, the equations for calculating profile lift and drag coefficients are integrated with those describing the momentum and blade/fluid interaction phenomena: the result is a procedure that does not require overly long iterations to take into account the effect of the actual values of the incidence angles and Reynolds number. The method is then applied to predict the performance of four Wageningen B-screw series propellers. Next, the

behavior of one of the previously examined screws is investigated by means of a three-dimensional viscous calculation with the aim of both comparing the results with those obtained using CMBET and establishing a comprehensive theory to understand the pros and contra of this approach. The purpose of such analysis is to give evidence that the blade element theory is still very significant in the framework of a procedure for preliminary propeller design and analysis.

## 2. Combined momentum-blade element theory

A relatively simple but effective method to predict the performance of a propeller is the use of the MBET along with the momentum theory (MT), as described in the early work by Rankine, Froude, Lanchester and Prandtl. The result is usually called the combined momentum-blade element theory (CMBET). As it is well known, in this method the propeller is divided into a number of elementary streamtubes (called “strips”) along the radius, where a force balance is applied involving two-dimensional profile lift and drag along with the thrust and torque produced within the strip (Fig. 1). At the same time, a balance of axial and angular

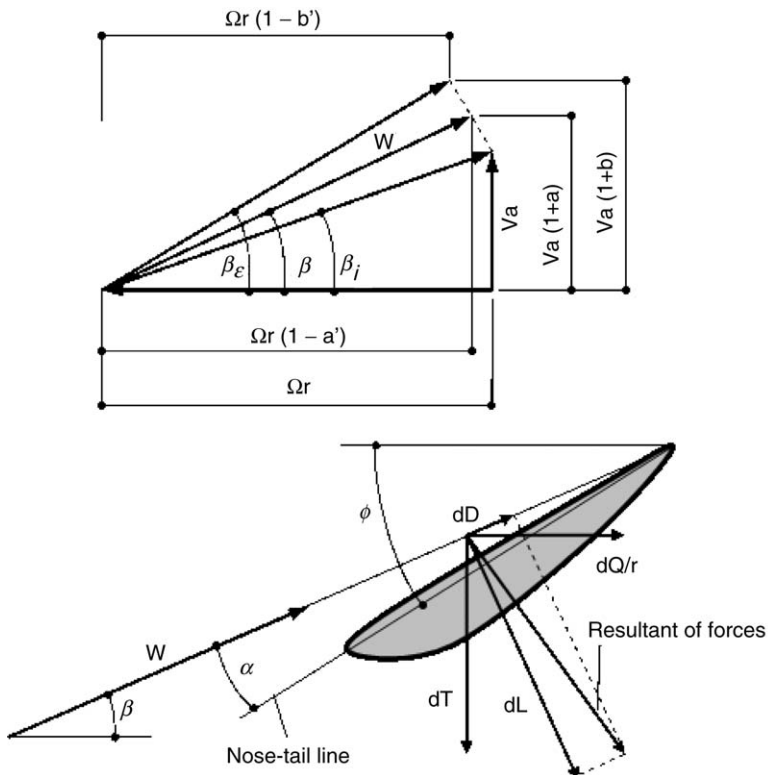


Fig. 1. Velocity triangles and forces on a blade element.

momentum is applied. This produces a set of non-linear equations that can be solved iteratively for each blade strip. The resulting values of elementary thrust and torque are finally integrated along the radius to predict the overall propeller performance. It is worth noting that the strip theory is fully analytical in its formulation, and this makes the model easy to implement and almost inexpensive to run.

In this paper, the CMBET follows the approach presented by Goldstein (1929), Betz (1919, 1920) and Tachmindji and Milan (1957), with however, an important difference regarding estimation of profile characteristics. In particular, the system of equations to be solved at each radial strip is the following:

$$dT = 0.5\rho W^2 Bc(C_L \cos\beta_i - C_D \sin\beta_i) dr \quad (1.1)$$

$$W^2 = V_A^2(1+a)^2 + \Omega^2 r^2(1-a')^2 \quad (1.2)$$

$$\tan\beta_i = \frac{1+a}{1-a'} \frac{V_A}{\Omega r} = \frac{\tan\beta + \tan\beta_e}{2} \quad (1.3)$$

$$\alpha = \phi - \beta \quad (1.4)$$

$$dT = 4\pi\rho r K_e V_A^2 a(1 + K_\beta a) dr \quad (1.5)$$

$$K = K(B, r/R, \beta_x) \quad (1.6)$$

$$V_A^2 a(1+a) = (\Omega r)^2 a'(1+a') \quad (1.7)$$

Once the local axial and tangential thrust have been calculated by solving the system of Eqs. (1.1)–(1.7) at each radial strip, the overall thrust produced and torque absorbed by the propeller can be obtained by integrating the elementary components along the radius

$$T = \int_{r_{\text{boss}}}^R dT; \quad Q = \int_{r_{\text{boss}}}^R dQ = \int_{r_{\text{boss}}}^R 0.5\rho W^2 Bc(C_L \sin\beta_i + C_D \cos\beta_i) r dr \quad (2.1)$$

The performance coefficients are finally derived as usual:

$$K_T = \frac{T}{\rho n^2 D^4}; \quad K_Q = \frac{Q}{\rho n^2 D^5}; \quad \eta = \frac{J}{2\pi} \frac{K_T}{K_Q} \quad (3.1)$$

The screw profiles' performance is usually derived from the results obtained using wind- or water-tunnel tests on two-dimensional airfoils. However, these results refer typically to infinite-length airfoils at given Reynolds numbers and must be corrected before being applicable to propellers. In fact, the influence of a finite height on a blade operating at arbitrary Reynolds number is usually accounted for using empirical corrections. The accuracy of such corrections is doubtful in the majority of cases and leads to erroneous predictions, especially when applied to non-conventional airfoils families for which no correlations are available. This fact holds in particular for the estimation of the cavitation margin, being a complex function of the profile shape and operating conditions. In this respect, the use of empirical models in CMBET should be avoided and, in any case, limited as much as possible.

An alternative way to predict the lift, drag and pressure distribution on a blade element is used in this paper. In particular, a two-dimensional IBLM is employed. Using this method, it is possible to quickly compute the performance of profiles taking into account the actual shape under the real operating conditions. Consequently, empirical corrections for Reynolds number are no longer needed. In the CMBET, the above cited IBLM can be implemented in a straightforward way, and makes it possible to obtain a fast and accurate prediction tool.

The IBLM used here is implemented in XFOIL, a coupled panel/viscous code developed at MIT (Drela and Giles, 1987; Drela, 1989a,b). XFOIL is a collection of programs for airfoil design and analysis for incompressible/compressible viscous flows over an arbitrary airfoil. In this code, a zonal approach is used to solve the viscous flow indirectly and an equivalent inviscid flow is postulated outside a displacement streamline that includes the viscous layer. Fig. 2 reports the comparison between measured and computed results regarding lift and drag coefficients of two modified NACA 66 profiles, i.e. 663418 and 66206 taken from Abbott and von Doenhoff (1958), obtained using 120 panels for geometry discretization of blade profile and a Reynolds number of  $3 \times 10^6$ . The results confirm the capability of the code to give accurate predictions on two-dimensional flows around an airfoil. Regarding the profile NACA 663418, for example, the code accuracy is good over the entire range of incidence angles that usually occur in propellers (i.e. from  $+4^\circ$  to  $-4^\circ$ ), while the predictions get poorer away from this condition (e.g. a discrepancy of about 15% have been registered when  $\alpha = -10^\circ$ ). It is worth noting that the code was able to capture the deflection of the lift coefficient in the range from  $7^\circ$  to  $8^\circ$  of the incidence angle. The accuracy of the code was confirmed in the analyses of the profile NACA 66206, where the discrepancies between experimental and calculated data never exceed 5% in the range  $\alpha = [-4^\circ + 4^\circ]$ . The calculated pressure distribution at a given incidence angle is rather well predicted: only in the region close to the leading edge, and between 80% and 90% of the chord length greater values of pressure were registered. However, this discrepancy, which may be caused by the uncertainties in the actual value of surface roughness, does not

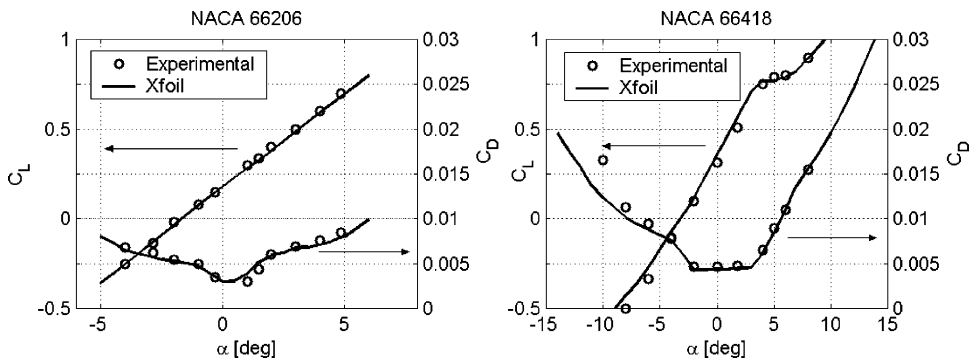


Fig. 2. Comparison between experimental and predicted performance of propeller airfoils.

affect the estimation of the profile lift in a significant way since the area of pressure within the suction and pressure sides is approximately unvaried.

The CMBET was implemented on a personal computer and the solution scheme to obtain the screw performance is indicated in Fig. 3. For each radial strip, a loop is performed to obtain the values of the unknown variables of the system Eqs. (1.1)–(1.7). First of all, a tentative value for  $a$  is postulated; using this value, a first group of unknown variables ( $a'$ ,  $\beta_i$ ,  $W_\infty$ , and  $\alpha$ ) are calculated in sequence

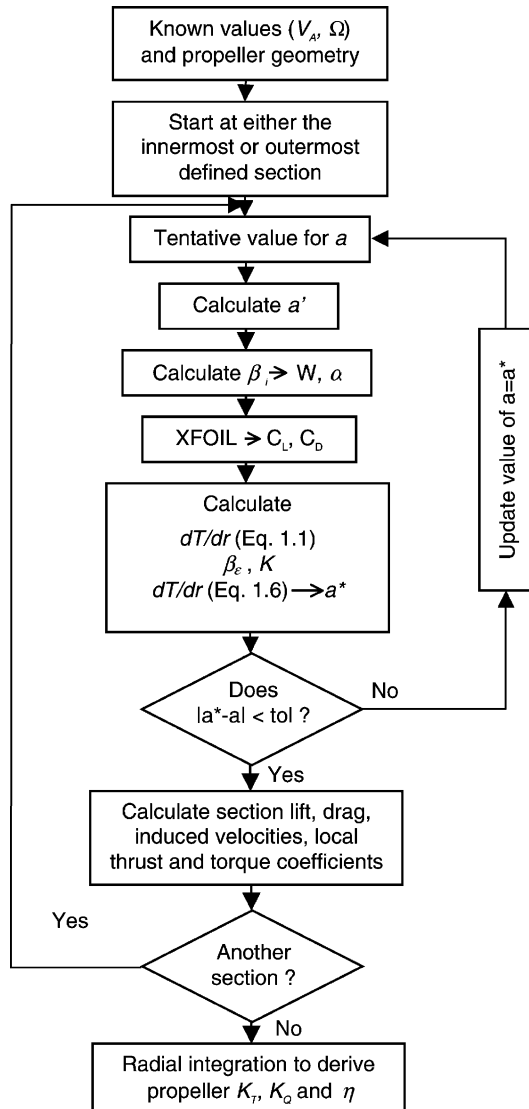


Fig. 3. Propeller performance calculation scheme.

from Eqs. (1.7), (1.3), (1.2) and (1.4), respectively. Next, the actual profile lift and drag coefficients are estimated as functions of the incidence angle and Reynolds number using XFOIL and, then, used to calculate the local value of the thrust (Eq. (1.1)), the outflow angle  $\beta_e$  (right-hand side of Eq. (1.3)) and the Goldstein–Tachmindji correction factor  $K$  (Eq. (1.6) is given in tabulated form by Carlton (1994)). Finally, a new value of  $a$  (named  $a^*$ ) is determined using Eq. (1.5) and compared to the value assumed at the beginning of the iteration: if the difference falls within a predefined tolerance, the section forces as well as induction factors and local thrust and torque coefficients are calculated and stored, and another strip is considered; if not, the value of  $a^*$  is adopted as the current value for  $a$  and the process starts again until the convergence criterion is satisfied.

### 3. Application of CMBET to performance prediction of 3-bladed Wageningen screws

The proposed CMBET method was applied to predict the open-water characteristics of four 3-bladed Wageningen B-series screws (Troost, 1938, 1940, 1951; Lammeren et al., 1969) having a blade-area ratio of 0.5, these four geometries corresponding to different values of the pitch ratio ( $P/D = 0.6, 0.8, 1.0$  and  $1.2$ ). The Wageningen series was chosen being a well known test case, the behavior of which has been deeply studied in the past, and which is currently representative of general purpose fixed-pitch propeller design. Rotational speed was fixed at 34.6958 rad/min, while the undisturbed velocity  $V_A$  was varied in order to obtain different values of the advance coefficient  $J$ . The propeller blade was divided radially into eight strips (from  $r/R = 0.18$  to  $r/R = 0.95$ ): these strips were equally spaced ( $\Delta r/R = 0.10$ ) except the one adjacent to propeller boss ( $\Delta r/R = 0.07$ ). The outmost portion of the blade ( $r/R > 0.95$ ) was not modeled and its effect on blade thrust and torque neglected.

The performance of the Wageningen propellers were calculated using the polynomials provided by Oosterveld and Oossanen (1975), which are based on accurate regression analyses from experimental data on propeller models. A comparison between the results obtained from such calculation and those derived from the application of the CMBET is given in Fig. 4. As a general indication, the accuracy in the prediction of propeller performance using CMBET depends on the value of the advance coefficient  $J$ . In particular, when  $J$  is close to its minimum value, both the thrust and torque coefficients are underestimated while an opposite behavior is recorded at high values of  $J$ . As a result, the propeller efficiency is very well predicted at the lowest  $J$  but tends to be more and more over predicted as  $J$  increases. As a matter of fact, there exists a value of  $J = J^*$  where the CMBET gives extremely accurate predictions and this value depends on the geometry of the propeller. For the B3-50 propeller, i.e. the one considered here, such value increases from  $J^* = 0.2$  to  $J^* = 0.9$  as the pitch ratio changes from 0.6 to 1.2, respectively. These values of  $J^*$  are in fact those that approximately correspond to the propeller “nominal operation”. The farther one moves from  $J^*$ , the greater the error in the



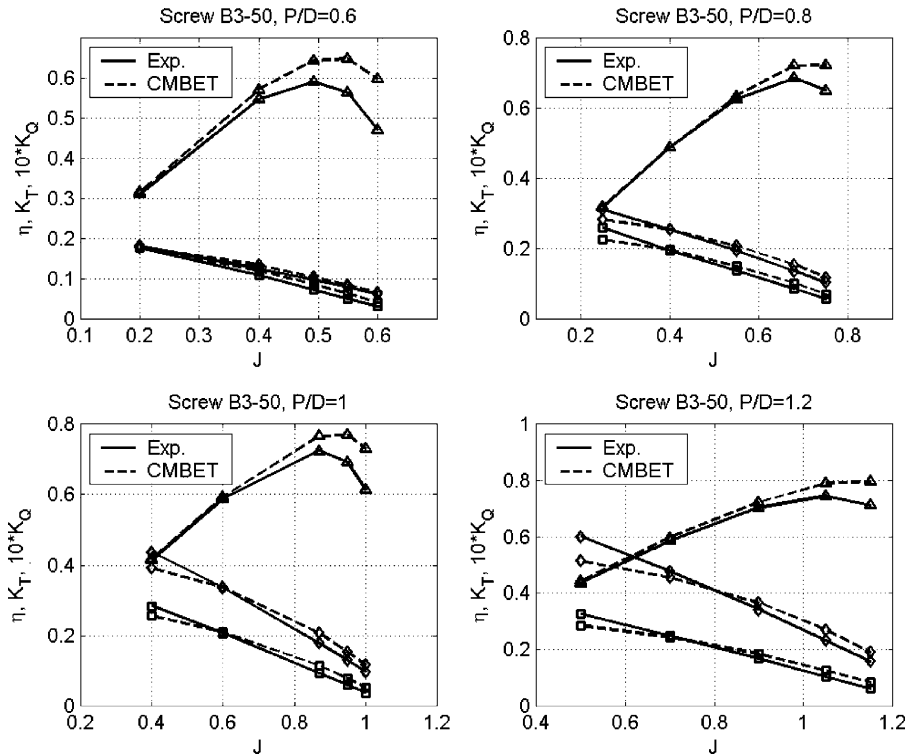


Fig. 4. Comparison between experimental and predicted performance of Wageningen B-screw series propellers.

performance prediction using CMBET. The reasons of this discrepancy are attributable to three-dimensional effects and are discussed in the next section, where a comparison between the results obtained using CMBET and a three-dimensional Navier–Stokes code is presented.

#### 4. Three-dimensional Navier–Stokes calculations

The behavior of the Wageningen B3-50 ( $P/D = 1$ ) propeller was investigated as a function of  $J$  by means of a fully three-dimensional Navier–Stokes calculation using the commercial CFD code Fluent 6.0<sup>™</sup> by Fluent Inc. A multi block-structured grid was constructed for this purpose (using the package GAMBIT 2.0) that represents a circumferential portion ( $120^\circ$ , i.e. one 1/3 of the round angle, owing to the axis-symmetrical nature of the problem) of the streamtube upstream and downstream of the propeller, as well as the region outside this streamtube that extends toward the far field (Fig. 5). For simplicity and following an explicit intention to not introduce any influence of three-dimensional shape of the hub, the actual geometry of propeller boss was not represented: a cylinder passing through

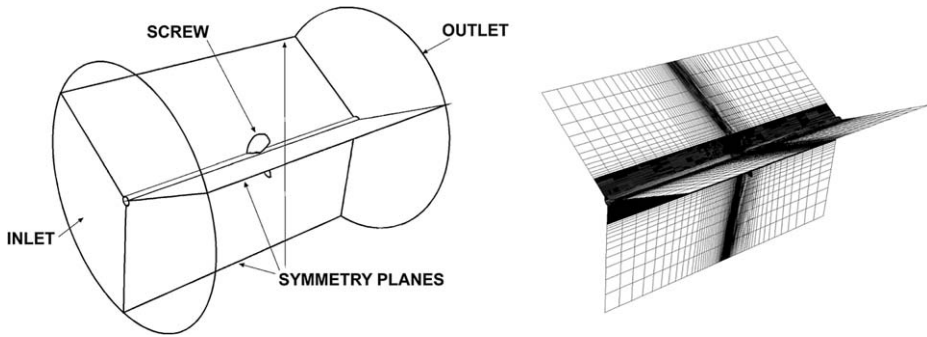


Fig. 5. Computational domain and grid for three-dimensional Navier–Stokes calculations.

the whole fluid region simulated the presence of an ideal shaft of infinite-length (a no-slip condition was applied to the shaft wall). The flow domain contains approximately 800,000 nodes, 20,000 of which are positioned on propeller blade surface (Fig. 6). Using such grid topology, it was not possible to model the peripheral region of the blade exactly because the grid cells would have collapsed toward the tip. For this purpose, the outmost part of blade was “cut” using a cylindrical surface at 99.5% of the original propeller radius.

Boundary conditions were applied as follows. As mentioned before, the surface corresponding to the imaginary shaft was given a wall condition with no-slip. At the inlet of the flow domain, a “velocity-inlet” condition was applied that corresponded to the desired undisturbed velocity being simulated. At the outlet, a “pressure-outlet” condition was established that matched a static relative pressure

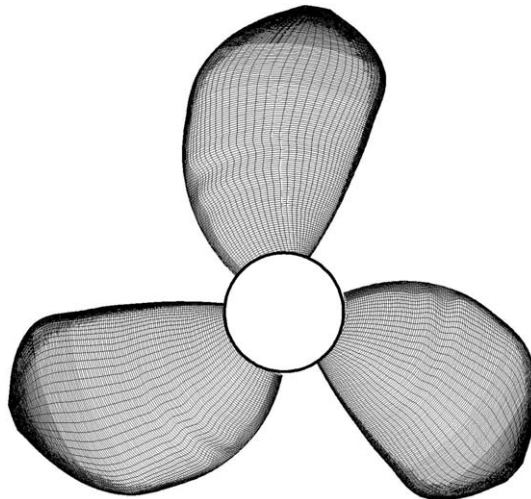


Fig. 6. Computational grid of Wageningen B3-50 propeller.

equal to 0. The lateral surface was given a “symmetry” condition. All the wall surfaces, including those of the blade, were assumed to be ideally smooth (i.e. with a relative roughness equal to 0). A standard  $k-\varepsilon$  turbulence model was used along with standard wall functions to solve the boundary layer. No cavitation model was activated.

Computed results of overall propeller performance are given in Fig. 7, where experimental and CMBET results have been included for quick reference. A good agreement between Navier–Stokes calculations and experiments was achieved over the operating range of the propeller: contrary to the CMBET, the three-dimensional calculation gave reliable results independent from  $J$ , the maximum discrepancy from experimental results being in the order of 5% in the prediction of  $K_T$ ,  $K_Q$  and  $\eta$ .

The results of the three-dimensional calculations were then used to establish a theoretical basis for understanding the flow physics at various operating conditions and for discerning the limitations of the CMBET model. However, it must be recognized that the interpretation of such results is very complex and perhaps possible only taking into account several phenomena, which occur simultaneously. Some of these phenomena are of primary importance in the purpose here since they make it possible to isolate the sources of three-dimensional flows: they involve

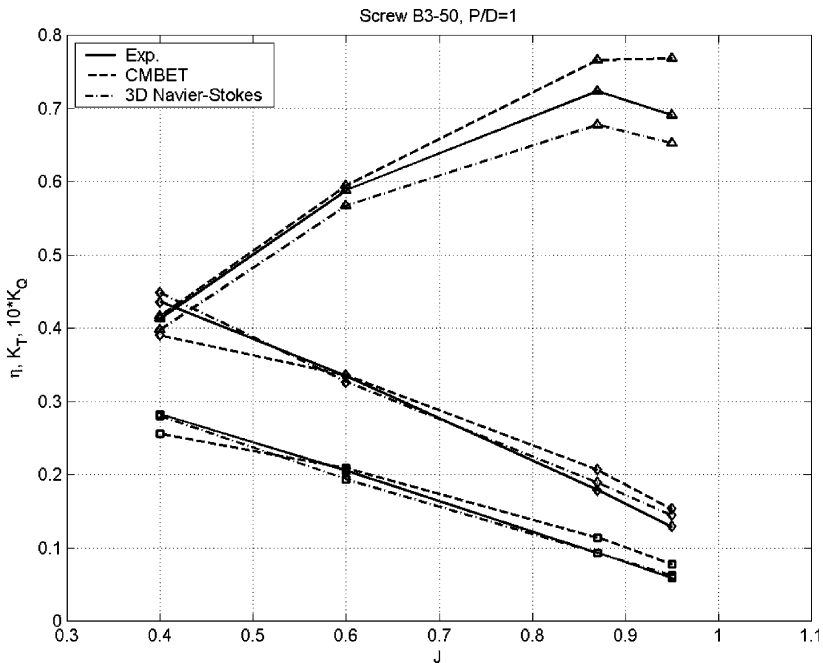


Fig. 7. Comparison between experimental and predicted performance (using CMBET and three-dimensional Navier–Stokes calculations) of Wageningen B-screw series propellers.

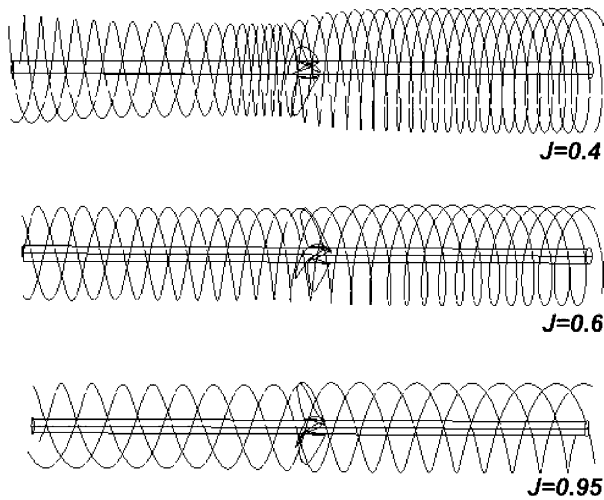


Fig. 8. Particle tracks at different values of the advance coefficient.

streamtube contraction caused by change in the axial momentum, tip vortex flows and radial equilibrium condition among individual streamtubes, as outlined below.

Fig. 8 shows how the lagrangian trajectory of a generic fluid particle, passing through the B3-50 propeller blade in a region close to the tip, changes as a function of  $J$ . When  $J$  is small, i.e. when  $V_A$  is small compared to the blade tangential speed, the contraction of the streamtube intercepting the rotor is obviously more evident and this contributes to originate three-dimensional effects, the most noticeable of which is the appearance of a negative radial component of the flow velocity  $V_r$  (i.e. directed from the tip to the boss) at the blade tip, which is represented also in Fig. 9 on a set of blade-to-blade surfaces. Another significant contribute to the onset of  $V_r$  comes from the tip vortex flow, because the tip profiles are highly loaded (see distribution of the pressure coefficient, Fig. 10), but in this case this component moves outboard, i.e. is positive (see nuclei of  $+V_r$  close to leading edge of the tip blade). The absolute value of  $V_r$  becomes small over the rest of the blade, as a consequence of the effectiveness in the radial equilibrium between the elementary streamtubes along the span, and because the tip vortex flows inevitably reduce moving toward to boss.

As one might expect, the values of  $V_r$  reduce when  $J$  gets closer to  $J^*$  (Fig. 11) as a result of both the reduction in the overall streamtube contraction (Fig. 8) and of the effective radial equilibrium; also in this case the incidence angles are positive over the largest part of the blade (Fig. 15) but of lesser entity compared to the situation at smaller  $J$  (as demonstrates the distribution of the pressure coefficient as a function of  $r/R$ , Fig. 12). Therefore, the tip vortex flows tend to reduce and the flow remains well attached to the blade profile.

Radial components of flow velocity return to increase over the entire blade when  $J \gg J^*$ , being in fact in the same order of magnitude as the undisturbed velocity

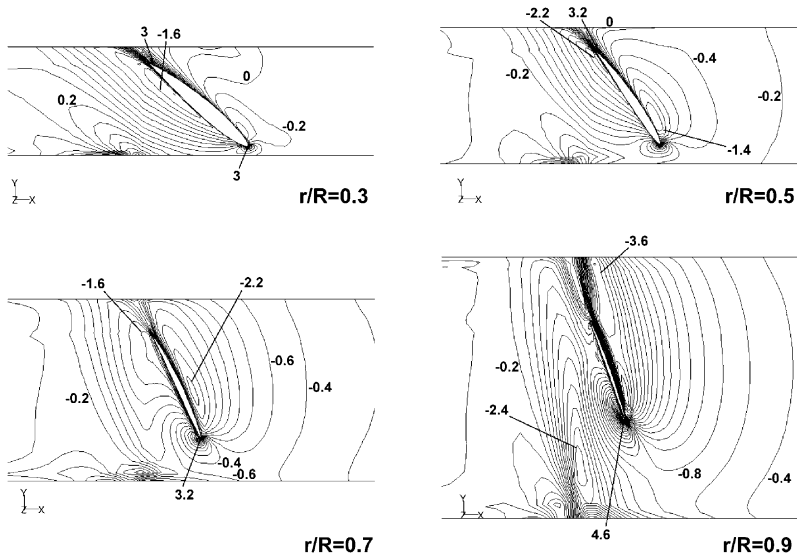


Fig. 9. Contour plots of the radial component of flow velocity on cylindrical surfaces at different radii ( $J = 0.4$ ).

when  $J = 0.95$  (Fig. 13), as a consequence of the unsuccessful radial equilibrium between the centrifugal and the pressure force. In fact, in these conditions the flow intercepts the blade with almost negligible contraction (Fig. 8) but with massive

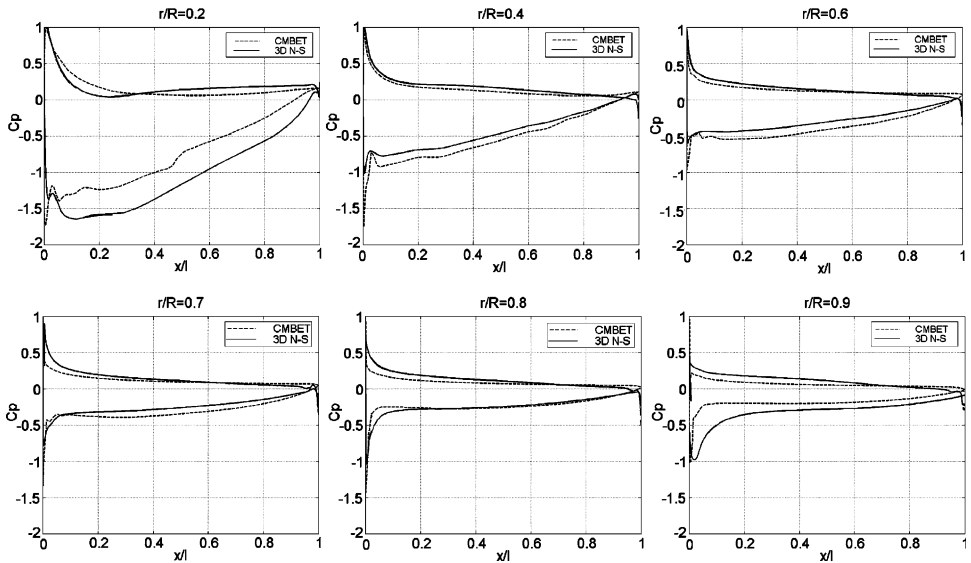


Fig. 10. Spanwise distribution of pressure coefficient of propeller B3-50 ( $J = 0.4$ ).

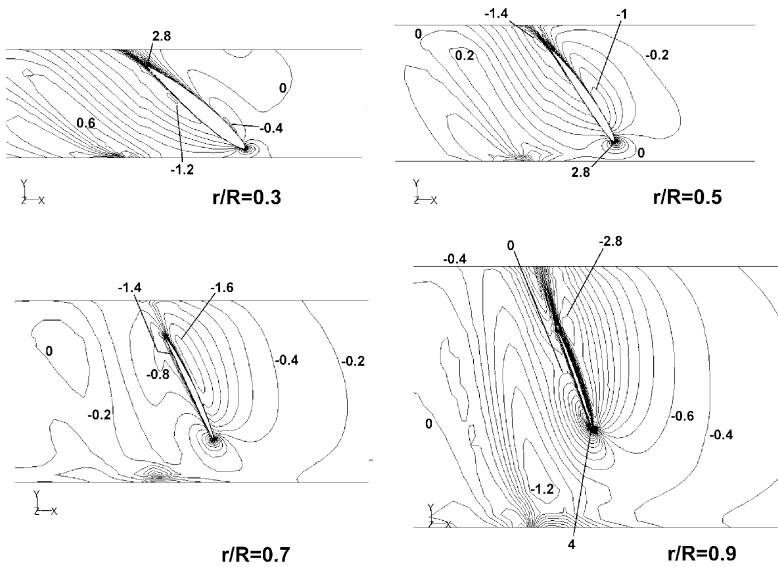


Fig. 11. Contour plots of the radial component of flow velocity on cylindrical surfaces at different radii ( $J = 0.6$ ).

negative incidence angles (Fig. 15), especially in the central part of the blade. As a result, low momentum fluid particles migrate from the blade tip to the center following the imbalance between the pressure and the centrifugal force within the

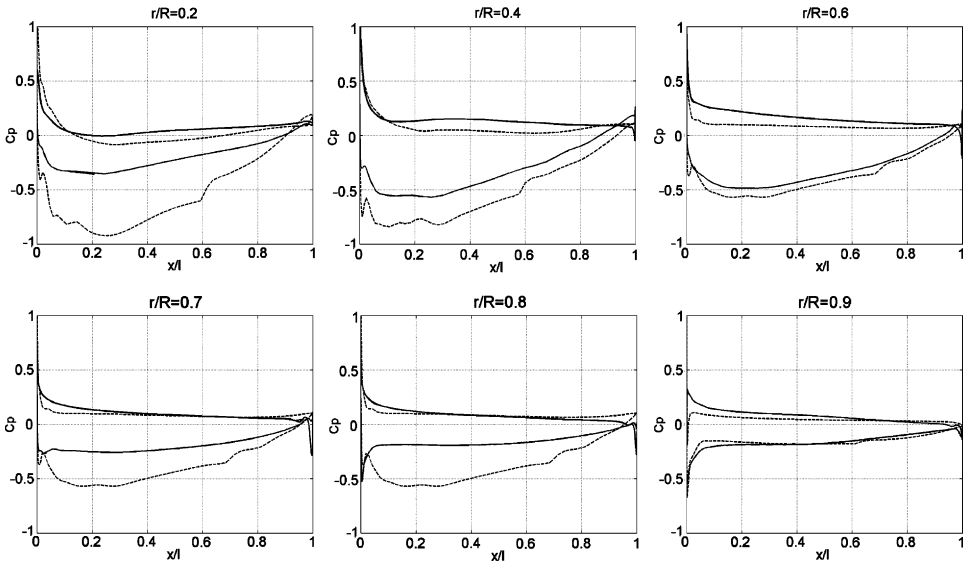


Fig. 12. Spanwise distribution of pressure coefficient of propeller B3-50 ( $J = 0.6$ ).

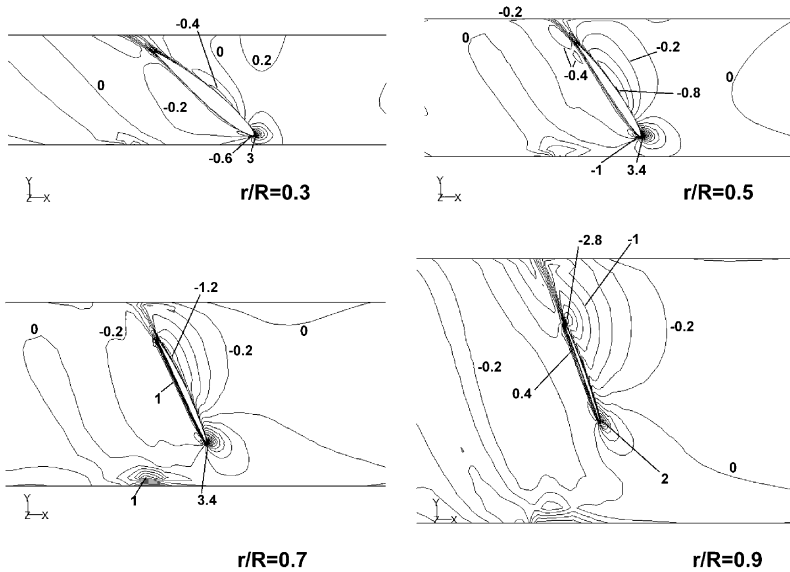


Fig. 13. Contour plots of the radial component of flow velocity on cylindrical surfaces at different radii ( $J = 0.95$ ).

blade. Also, it is worth noting that in these conditions tip vortex flows considerably reduce following the diminution in the blade loading (Fig. 14).

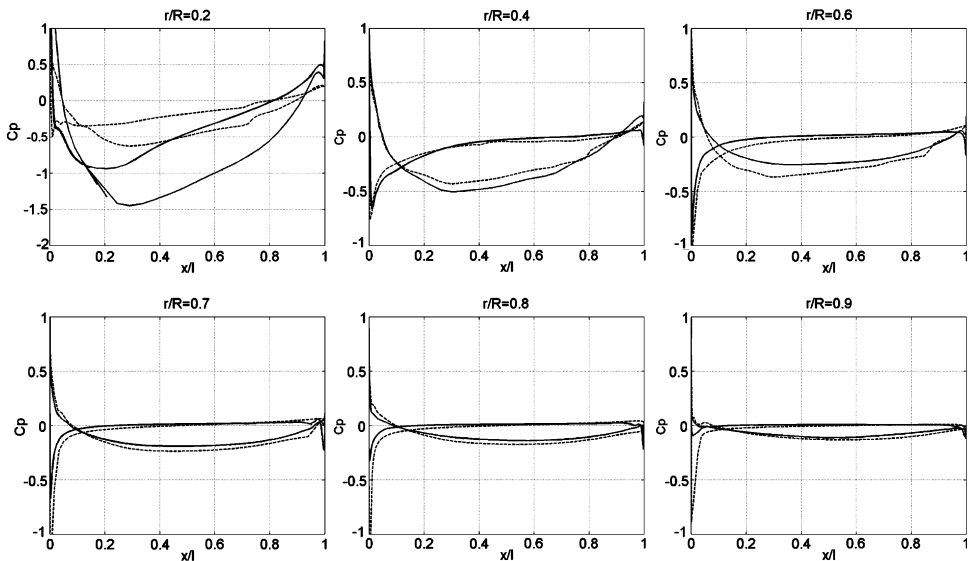


Fig. 14. Spanwise distribution of pressure coefficient of propeller B3-50 ( $J = 0.95$ ).

To summarize, when  $J \neq J^*$  the flow can no longer be considered two-dimensional: for  $J \ll J^*$  the contraction of the overall streamtube and tip vortex flows generate considerable radial flow at the tip while, when  $J \gg J^*$  the phenomenon is dominated by the presence of non-equilibrium flows in the radial direction. However, the overall propulsion efficiency tends to increase when  $J \gg J^*$ , as a consequence of the well known propulsive effect linked to the reduction in the axial momentum with  $J$  (impulsive phenomenon), which has a positive influence on  $\eta$ , and over compensates the natural decrement in the blade efficiency caused by over negative incidence angles. In fact, in these propellers the maximum propulsion efficiency is located at values of  $J$  where the thrust is close to zero.

### 5. Comparison between CMBET predictions and three-dimensional simulations

The results obtained from the three-dimensional calculations confirmed that the prediction of propeller performance using CMBET is accurate only when  $J$  is close to  $J^*$ , i.e. when the three-dimensional effects are of secondary importance. The purpose here is to give a quantitative justification of the difference between the results obtained using the two approaches when  $J$  is far from  $J^*$ .

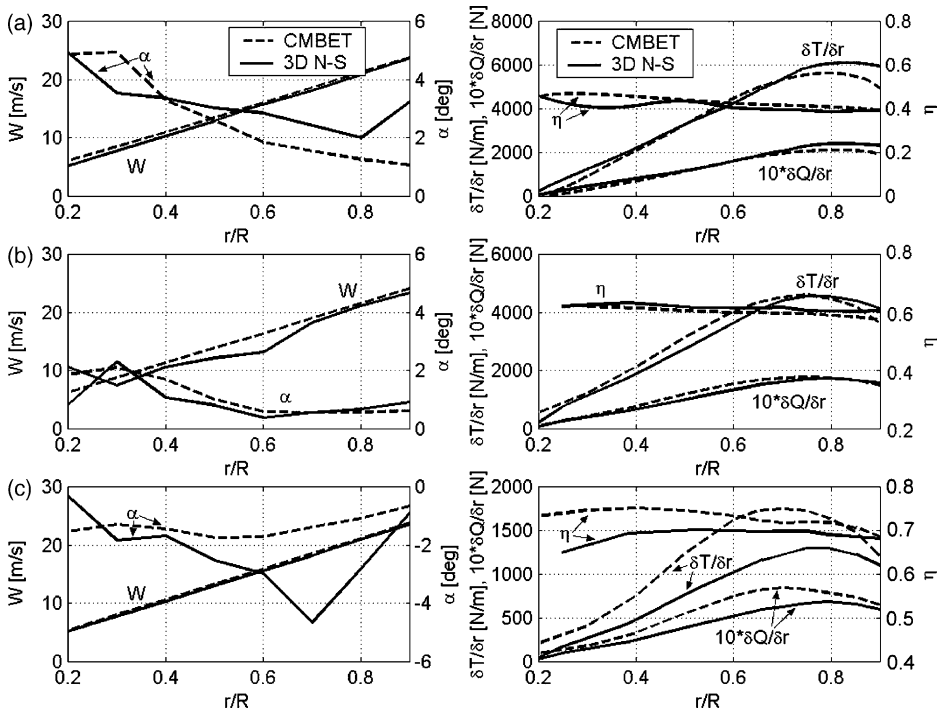


Fig. 15. Radial plots of propeller characteristics. (a)  $J = 0.4$ , (b)  $J = 0.6$ , (c)  $J = 0.95$ .



Fig. 15 shows a comparison between some of the most influencing quantities on predicted performance obtained using CMBET and three-dimensional simulations as a function of  $J$ . These include the values of the incidence angle  $\alpha$ , the relative velocity  $W$ , as well as the distribution of elementary thrust  $dT/dr$  and torque  $dQ/dr$  in the radial direction. From this figure, it appears that the CMBET is able to predict the absolute value of the relative velocity quite well in all the conditions, while the major discrepancies compared to three-dimensional simulations regard the incidence angle. This is under predicted over the largest part of the blade when  $J$  is small, leading to a smaller overall thrust and torque (Fig. 7), and is over predicted when  $J$  is large, resulting in an apposite influence on performance. Since  $K_T$  increases more than  $K_Q$  as a function of  $J$ , the efficiency tends to be more and more over predicted as  $J$  increases. This is confirmed also by the radial plots of  $dT/dr$  and  $dQ/dr$  in Fig. 15: in fact the elementary thrust is more and more over predicted as  $J$  increases, see Eq. (1.1). From these results, it can be concluded that the major source of errors within the CMBET relies on the poor prediction of the incidence angles as functions of  $J$ .

## 6. Conclusions

A new implementation of the CMBET theory based on a numerical estimation of the actual performance coefficients of blade profiles was presented and tested to predict the characteristics of a family of Wageningen B-screw series propellers. The results revealed that the accuracy of such predictions are very sensitive to  $J$ , the minimum error being in the order of less than 2% when  $J$  falls within a neighborhood of the nominal value  $J^*$ , which perhaps coincides with the design condition. A three-dimensional model of one of the above mentioned propellers was carried out and validated against experimental data to establish a theoretical basis upon which to interpret the results obtained using CMBET, which is intrinsically two-dimensional. The main reason for the discrepancies between the two approaches relies on the poor prediction, obtained from CMBET, of the incidence angles as functions of  $J$ , being this caused by the onset of three-dimensional effects, the intensity of which is more and more important as  $J$  moves away from  $J^*$ . However, when  $J$  falls within a neighborhood of  $J^*$ , the results obtained using CMBET are very accurate.

In conclusion, the significance of the CMBET approach is considerable, compared to other more complex analysis techniques, for design purposes of marine propellers because it is very simple, fast and almost inexpensive to implement and run on a common personal computer. In this way, an application of the CMBET in the framework of optimizing the propeller geometry at the design point is valuable and reasonably straightforward.

## References

Abbott, I.H., von Doenhoff, A.E., 1958. Theory of Wing Sections. Dover Publications, Inc, New York.

- Betz, A., 1919. *Ergebn. Aerodyn. Vers Anst Gottingen*.
- Betz, A., 1920. Eine Erweiterung der Schrauben Theorie. *Zreits, Flugtech.*
- Black, S.D., 1997. Integrated lifting-surface/Navier–Stokes design and analysis methods for marine propulsors, Ph.D. Thesis. Massachusetts Institute of Technology.
- Carlton, J.S., 1994. *Marine Propellers and Propulsion*. Butterworth-Heinemann Ltd.
- Chen, B., Stern, F., 1999. Computational fluid dynamics of four-quadrant marine-propulsor flow. *Journal of Ship Research* 43 (4), 218–228.
- Drela, M., 1989a. Integral boundary layer formulation for blunt trailing edges. Paper AIAA-89-2200.
- Drela, M., 1989b. XFOIL: an analysis and design system for low Reynolds number airfoils. In: *Conference on Low Reynolds Number Airfoil Aerodynamics*, University of Notre Dame, June 1989.
- Drela, M., Giles, M.B., 1987. Viscous–inviscid analysis of transonic and low Reynolds number airfoils. *AIAA Journal* 25 (10), 1347–1355, (October).
- Feng, J., Wang, L., Ahuja, V., Lee, Y.T., Merkle, C.L., 1998. CFD modeling of tip vortex for open marine propellers. In: *Proceedings of the 1998 ASME Fluids Engineering Division Summer Meeting*, 21–25 June 1998, Washington, DC, USA.
- Goldstein, S., 1929. On the vortex theory of screw propellers. *Proceedings of the Royal Society, Series A* 123.
- Hsiao, C.T., Pauley, L.L., 1998. Numerical computation of tip vortex flow generated by a marine propeller. In: *Proceedings of the 1998 ASME Fluids Engineering Division Summer Meeting*, 21–25 June 1998, Washington, DC, USA.
- Lammeren, W.P.A., van Manen, J.D., Oosterveld, M.W.C., 1969. The Wageningen B-screw series. *SNAME Transactions* 77.
- Martinez-Calle, J., Gonzalez-Perez, J., Balbona-Calvo, L., Blanco-Marigorta, E., 2002. An open water numerical model for a marine propeller: a comparison with experimental data. In: *Proceedings of the 2002 ASME Joint U.S.–European Fluids Engineering Conference*, 14–18 July 2002, Montreal, Que., United States, pp. 807–814.
- Oosterveld, M.W.C., van Oossanen, P., 1975. Further computer-analyzed data of the Wageningen B-screw series. *International Shipbuilding Progress* 22, 251–262.
- Tachmindji, A.I., Milan, A.B., 1957. The calculation of the circulation for propellers with finite hub having 3, 4, 5 and 6 blades. D.T.M.B. Report no. 1141.
- Troost, L., 1938. Open-water test series with modern propeller forms. *Transactions NECIES* 54, (Also NSMB No. 33, Wageningen, The Netherlands).
- Troost, L., 1940. Open-water test series with modern propeller forms. *Transactions NECIES* 56.
- Troost, L., 1951. Open-water test series with modern propeller forms. *Transactions NECIES* 67.